JOURNAL OF GEOPHYSICAL RESEARCH, VOL. 101, NO. C3, PAGES 6377–6391, MARCH 15, 1996

Current structure of the south Indian Ocean

Michael D. Sparrow and Karen J. Heywood

School of Environmental Sciences, University of East Anglia, Norwich, England

Juan Brown

Ministry of Agriculture, Fisheries and Food, Directorate of Fisheries Research, Fisheries Laboratory Lowestoft, England

David P. Stevens

School of Mathematics, University of East Anglia, Norwich, England

Abstract. Using recently published atlas data [*Olbers et al.*, 1992] and the Fine Resolution Antarctic Model (FRAM) [*Webb et al.*, 1991], an investigation has been conducted into the structure of the frontal jets centered around the region of the islands of Crozet (46°27'S, 52° 0'E) and Kerguelen (48°15'S, 69°10'E) in the south Indian Ocean. Geostrophic current velocities and transports were calculated from the temperature and salinity fields available from the atlas and compared with results from FRAM and previous studies. We have identified the Agulhas Return Front (ARF) and the Subtropical Front (STF), as well as the following fronts of the Antarctic Circumpolar Current (ACC): the Subantarctic Front (SAF), the Polar Front (PF), and the Southern ACC Front (SACCF), from temperature and salinity characteristics and from geostrophic currents. This analysis of model and atlas data indicates that the jets associated with the ARF, STF, and SAF are topographically steered into a unique frontal system north of the islands, having some of the largest temperature and salinity gradients anywhere in the world ocean. The frontal jet associated with the ARF is detectable up to 75°E and has associated with it several northward branching jets. The PF bifurcates in the region of the Ob'Lena (Conrad) seamount; subsurface and surface expressions are identified, separated by as much as 8° of latitude immediately west of the Kerguelen Plateau. The surface expression, carrying the bulk of the transport (~65 Sv), is steered through the col in the Kerguelen Plateau at 56°S, 6° south of the latitude normally associated with the PF at this meridian. On crossing the plateau it rejoins the subsurface expression. In the south, passing eastward along the margin of the Antarctic continent and through the Princess Elizabeth Trough, a frontal jet is identified transporting up to 35 Sv, believed to be the SACCF [*Orsi et al.*, 1995], placing the southern extent of the ACC in the region at 67°S.

1. Introduction

In this paper we discuss the position and character of jets associated with frontal regions in the south Indian Ocean, in particular, the area around the islands of Crozet (46°27'S, 52° 0'E) and Kerguelen (48°15'S, 69°10'E) (Figure 1). Several frontal systems exist in the south Indian Ocean, the largest of which forms the Antarctic Circumpolar Current (ACC). The ACC is associated with several main frontal jets, which are primarily responsible for its eastward mass transport, the extent of which is usually defined in terms of the circumpolar waters that pass through Drake Passage (see *Orsi et al.* [1995] for a detailed description). Further details on the structure in Drake Passage and the South Atlantic are given by *Peterson and Stramma* [1991], *Read et al.* [1995], *Nowlin and Clifford* [1982], *Nowlin et al.* [1977], *Sievers and Nowlin* [1984], and *Nowlin and Klinck* [1986]. Reported observations from the south Indian Ocean are relatively sparse (e.g., the R/V *Conrad* cruise of 1974 [*Jacobs and Georgi*, 1977] and the early *Discovery* cruises [*Deacon*, 1937]).

Robertson and Watson [1995] indicated that the surface expression of frontal zones play a significant role as a source of atmospheric carbon dioxide (CO_2) in the south Indian Ocean, at least during austral summer, contrasting with the majority of the region which represents a sink. Knowledge of the fronts is important when determining the atmospheric CO_2 balance of the region.

The major fronts to the north of the ACC in the south Indian Ocean are the Agulhas Return Front (ARF) and the Subtropical Front (STF). The ARF is the southern rim of the circulation formed by the Agulhas Retroflection Return Currents [*Peterson and Stramma*, 1991] and the South Indian Ocean Current [*Stramma*, 1992], enclosing the warm and salty thermocline waters of the subtropical gyre in the south Indian Ocean. The STF, first observed by *Deacon* [1937], separates subtropical surface waters from Subantarctic Surface Water of the ACC. It is mainly a feature observed in the upper layers, with speeds decreasing rapidly with depth. On the basis of surface thermal characteristics from 89 ship crossings between 20°W and 60°E, *Lutjeharms and Valentine* [1984] calculated

Paper number 95JC03750.
0148-0227/96/95JC-03750$05.00

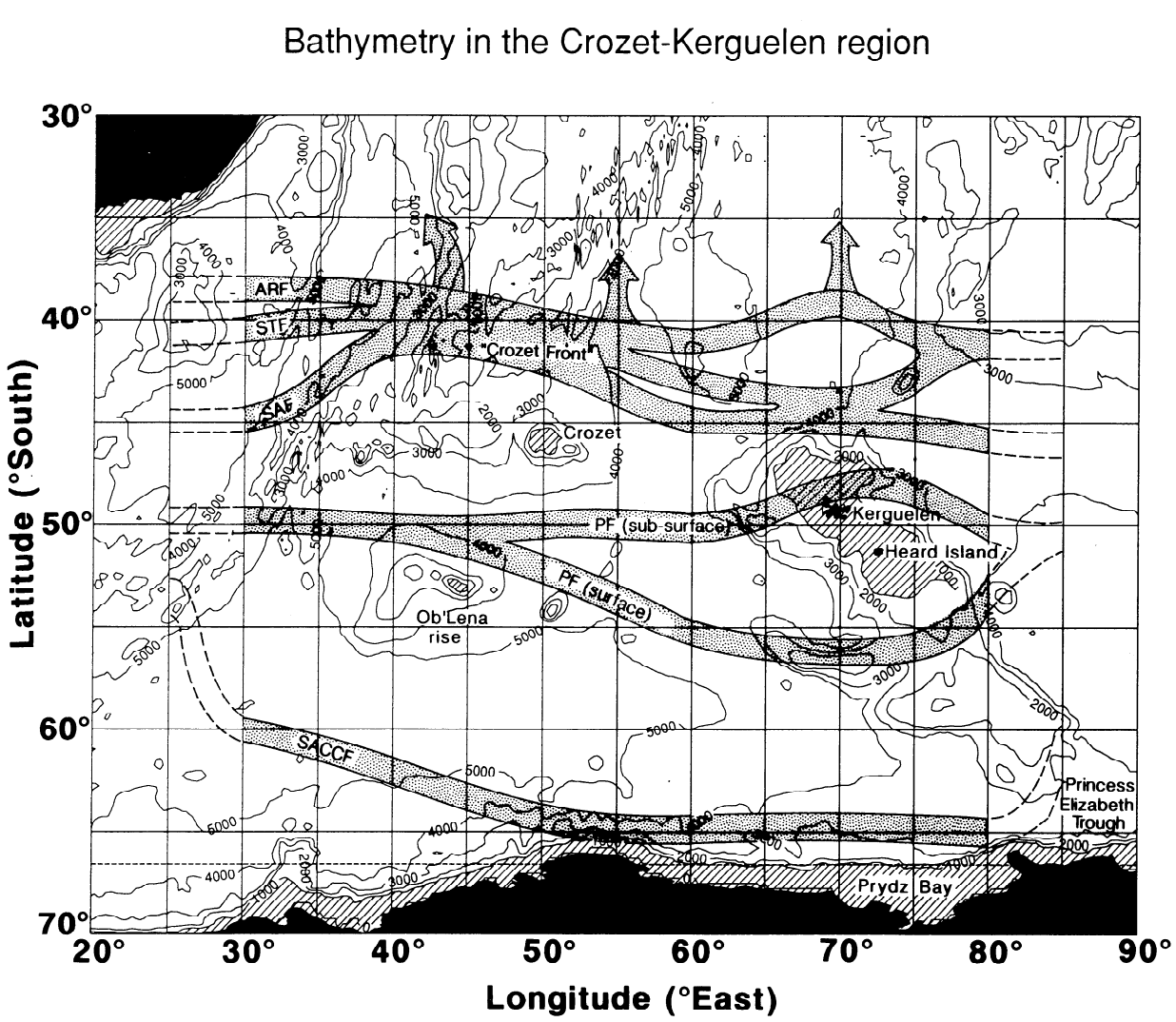

Figure 1. Bathymetry of the south Indian Ocean sector of the Southern Ocean. Contours are every 1000 m; areas shallower than 1000 m are shaded. Also shown is a schematic summary of the positions of the fronts determined from this analysis of the digital data set from the Hydrographic Atlas of the Southern Ocean (HASO) [Olbers et al., 1992].

the mean location of the STF to be 42°S, with a typical temperature decrease from north to south of 8.4°C and middle temperature of 14.3°C. *Whitworth and Nowlin* [1987] describe the STF by horizontal surface temperature and salinity transitions of 10-14°C and 34.6 to 35.1, respectively. We shall adopt a more precise form of this, suggested by *Orsi et al.* [1995], that the STF lies within a band across which temperatures increase northward from 10 to 12°C and salinities increase from 34.6 to 35.0 at 100 m. The ARF can either merge with or form a separate front to the north of the STF between 39 and 40°S. *Lutjeharms and Valentine* [1984] found the mean middle temperature of the ARF to be 18.4°C with a range of 15.7 to 21.0°C, though a temperature gradient between 12 and 16°C at 200 m is a more precise indication of its position [*Gordon et al.*, 1978] and one that we adopt.

The major recognized fronts of the ACC consist of the Subantarctic and Polar Fronts (SAF and PF) which form the northern and southern boundaries, respectively, of the Polar Frontal Zone (PFZ). Discussing the location of formation of Antarctic Intermediate Water (AAIW), *Whitworth and Nowlin* [1987] describe two fronts bordering the PFZ, the SAF to the north and the PF to the south. To the south of the PF is a pronounced minimum in temperature (~ -1.7°C) and salinity (~ 33.6) at approximately 100 m, characteristic of Antarctic Winter Water (WW), descending sharply to 300-400 m at the PF. Northward, in the PFZ, the temperature minimum remains distinct and gradually descends until the SAF, where it is found at 500-600 m. North of the SAF, in the Subantarctic Zone (SAZ), the temperature minimum is weak or absent. In the PFZ a salinity minimum is evident either at the surface or as a weak subsurface expression at ~200 to 300 m (i.e., slightly above the temperature minimum). The salinity minimum descends rapidly at the SAF and to the north forms the pronounced salinity minimum characteristic of AAIW. Although temperature and salinity definitions for the position of the SAF exist, they are dependent on the sector of the ocean under examination [*Peterson and Stramma*, 1991; *Belkin and Gordon*, 1996] and clearly, no definitive subsurface property values exist. In this analysis we use the structural definition of *Whitworth and Nowlin* [1987] and look for the rapid descent of the subsurface salinity minimum. The northern limit of the 2°C isotherm below 200 m is usually used to identify the

location of the subsurface expression of the PF [e.g., *Clifford*, 1983]. In some instances this is not coincident with the surface expression of the PF [*Lutjeharms and Valentine*, 1984], in which case the definition given by *Ostapoff* [1962], namely, that the PF lies where the maximum gradient of the sea surface temperature regime occurs between 2 and 6°C, is used. Throughout this analysis a further frontal structure south of the PF can be seen. We believe this is the same feature observed by *Orsi et al.* [1995], which they termed the Southern ACC Front (SACCF). In their study they found that the position of the SACCF coincided with particular property isolines, summarized below. Therefore we will compare the position of our southern frontal jet with the characteristics given by *Orsi et al.* [1995]. The southern limit of the SACCF coincides with the potential temperature θ being less than 0°C along a θ_{min} at depths less than 150 m. The northern limit is where θ is greater than 1.8°C along a θ_{max} at depths greater than 500 m or where the salinities are greater than 34.73 along S_{max} at depths deeper than 800 m. In addition, they noted that the boundary between the ACC and subpolar regime is sometimes associated with geostrophic shear (referred to as the southern boundary), the SACCF usually being found very close to this boundary [*Orsi et al.*, 1995].

The property indicators we shall adopt are summarized in Table 1. In some regions of the Southern Ocean, the ACC flow is constrained, most obviously at Drake Passage. Evidence from the Fine Resolution Antarctic Model (FRAM) [*Webb et al.*, 1991] and other models [e.g., *Webb*, 1993], as well as observational studies carried out in the Southern Ocean, suggest that the width of the ACC varies considerably with changing longitude [*Gordon et al.*, 1978; *Orsi et al.*, 1995] and that most of these changes are topographically induced. Topography has a major effect on flow structure. Flow can be completely blocked and forced to detour around topographic features or be forced northward or southward by mounts or depressions to conserve potential vorticity $(f + \xi) / H$, where f is planetary vorticity, ξ is relative vorticity, and H is the depth of the fluid. Away from coastal boundaries and other regions of large horizontal current shear, this may be approximated by f / H. Thus flow moving onto a plateau will be forced equatorward (H decreases, so f decreases), and flow encountering a topographic depression moves poleward; this is known as topographic steering.

Table 1. Property Indicators of Fronts

Frontal Structure	Adopted Criteria
Agulhas Return Front	θ change from 12 to 16°C at 200 m
Subtropical Front	θ change from 10 to 12°C at 100 m, S change from 34.6-35.0 at 100 m
Subantarctic Front	position of the rapid decent of the subsurface S minimum
Polar Front, surface	maximum gradient of SST regime between 2 and 6°C
Polar Front, subsurface	northern limit of the 2°C isotherm below 200 m
Southern ACC Front	$\theta > 1.8$°C along θ_{max} at $z > 500$ m, northern limit; $S > 34.73$ along S_{max} at $z > 800$ m, northern limit; $\theta < 0$°C along θ_{min} at $z < 150$ m, southern limit

SST is sea surface temperature.

Park et al. [1993] carried out a detailed hydrographic survey in the vicinity of the Crozet-Kerguelen Islands. They concluded that in the Crozet Basin area the ACC core forms a concentrated jet embedded within a narrow band of the frontal zone, formed by the confluence of the subtropical and subantarctic fronts. The confluence results from the northward deflection of the ACC as it crosses the Crozet Plateau and the subsequent merging with the Agulhas Return Current extension at the entrance of the Crozet Basin. Unfortunately, Park et al.'s conductivity-temperature-depth (CTD) sections only extended south to 51°S, so although they studied the current core to the north of Crozet and Kerguelen in some detail, they could say little of the flow farther south. Given the importance of the circumpolar circulation and comparative sparsity of reported observations in the south Indian Ocean, we have taken the opportunity offered by the recent publication of two Southern Ocean data sets to consider the spatial extent and structure of the circulation. The work complements and adds to two recent studies of the Southern Ocean by *Belkin and Gordon* [1996] and *Orsi et al.* [1995]. In the light of the recent World Ocean Circulation Experiment effort in the region, the study provides a background for more detailed observational work and enables a comparison of the flow structures derived from the *Hydrographic Atlas of the Southern Ocean* (HASO) and FRAM.

2. Analysis of Data Sets

The FRAM Atlas [*Webb et al.*, 1991] covers the Southern Ocean south of 24°S. It is based on the results of a general circulation model of the Southern Ocean [*The FRAM Group*, 1991]. Horizontal resolution is approximately 27 km, and there are 32 vertical levels which vary in thickness from 20 m at the surface to 233 m at depth. Thus the model is able to partially resolve eddies and fronts. The model was initialized as a cold (-2°C), saline (36.69), motionless fluid, and its temperature and salinity fields were relaxed toward the annual mean *Levitus* [1982] climatology for a 6-year period. Annual mean *Hellerman and Rosenstein* [1983] winds were increased linearly from zero to their full value during the third year of integration. The data in the printed atlas represent the state of the model after 6 model years. The integration was continued for a further 10 years. During this time the seasonal climatological winds of *Hellerman and Rosenstein* [1983] were used to drive the ocean at the surface and the relaxation to the Levitus climatology was switched off, except in the surface level. A model climatology was produced by averaging 72 monthly model dumps from the last 6 years of the integration. In summary, the model takes the climatological hydrography of Levitus and assimilates it to produce a dynamically consistent set of fields, namely, temperature, salinity and velocity. Thus, from a smooth initial climatology, a high-resolution database has been produced. As such, FRAM represents a nonconventional technique for examining the Southern Ocean. For this comparison with the other data

sets, the 6-year average data set was believed to be the most useful because short-lived features such as eddies are smoothed out. Temperature, salinity, and current velocity were extracted for the region between 20°E and 90°E and 30°S to 70°S.

HASO [*Olbers et al.*, 1992] is the most comprehensive compilation of historical hydrographic data in this region, containing about 38,000 hydrographic stations (Nansen bottle and CTD) occupied in the Southern Ocean since the early 1900's. Both gridded and ungridded data are available, but the former were used here, which consist of in situ temperature and salinity at 38 levels (0-5000 m) on a 1° by 1° grid. Temperature and salinity data were extracted for the region between 20°E and 90°E and 30°S to 70°S and used to calculate geostrophic currents relative to the deepest common level between station pairs.

3. Results

Figure 2 depicts surface velocity vectors in FRAM and derived from HASO. From FRAM the second depth level (32.35 m) was used since the surface level is modified by the inclusion of Ekman drift, which is absent in the geostrophic HASO calculations. To make identification of the frontal systems easier, sections of zonal transport (Figure 3) were calculated every 10° of longitude. The surface plot from FRAM is representative of much of the water column and at least the upper 1000 m. That is, the flow is self-similar in the vertical, with the velocity decaying with depth [*Killworth*, 1992]. Total zonal transports in the water column every 1° across the section (Figure 3b) were derived from the FRAM stream function. Using HASO (Figure 3a), the arrows represent the zonal baroclinic geostrophic transports in a 1° width of latitude. A selection of temperature, salinity, and velocity profiles is given to illustrate the analysis. In the discussion that follows, velocities and transports quoted are the zonal component, unless otherwise stated.

Section at 30°East

The 30°E section (Figures 2-5) between Africa and Antarctica can be considered remote from the topographic influence of the Crozet-Kerguelen region. In both the HASO and FRAM sections the Agulhas current and retroflection are easily identified to the south of Africa by their large velocities and transports. Defining the positions of the fronts from their temperature and salinity characteristics places the STF between 41 and 43°S and the ARF at about 40°S in HASO. The geostrophic velocities suggest that the STF and ARF have apparently merged, as there is no distinct delineation. The ARF/STF jet peak lies at 39°S, with a maximum eastward velocity of 23 cm s^{-1} (Figure 4c) and a transport of 95 Sv (1 Sv = 10^6 m^3 s^{-1}). The sinking of AAIW can best be observed in the subduction of the 34.4 isohaline, placing the SAF at 44-45°S and forming a weak but discernible jet distinct from that of the PF in the smoothed HASO section. South of Africa, some observations show the PF and SAF merging to form a single frontal structure [e.g., *Read and Pollard*, 1993; *Orsi et al.*, 1993], whereas others suggest the SAF is a separate feature [e.g., *Belkin and Gordon*, 1996; *Lutjeharms and Valentine*, 1984]. The inconsistencies may, in part, be attributed to differing temperature and salinity definitions for the front. South of Africa, *Belkin and Gordon* [1996] found the average temperature and salinity ranges to be 4.8-8.4 °C and 34.11-34.47, respectively, at 200 m, placing the SAF at 44-45°S in our analysis. The surface salinity minimum (Figure 4b) of 34.0 characteristic of the PFZ is evident. The PF can be observed at about 49°S, with an eastward geostrophic current of 20 cm s^{-1} at the surface. A further frontal jet can be identified at about 60°S, with a transport of 19 Sv. At this longitude its northern limit is colder by 0.2°C and less saline by 0.03 than *Orsi et al.*'s [1995] SACCF. This may be because at this longitude, the SACCF and the southern boundary are separated by several degrees of latitude and the geostrophic shear is associated with the Southern Boundary, rather than the SACCF, which may well be associated with the slight maxima in velocity and transport at 54.5°S (Figures 3a and 4). The total baroclinic transport relative to the bottom across this HASO section is 244 Sv (this includes the Agulhas Current and Retroflection).

In the dynamically sharpened FRAM the ARF and STF can be clearly seen as two separate frontal jets at 36.1°S and 39.4°S, with associated surface velocities of 39 and 44 cm s^{-1} (Figure 5c) and transports of 50 Sv and 79 Sv, respectively. This is confirmed by their temperature and salinity characteristics which place the fronts at 34-38°S and 39-40°S, respectively. The SAF is not easily identifiable and certainly forms no well-defined jet, though as there is no pronounced subsurface salinity minimum north of about 41°S, it may form a minor feature at this latitude. The PF forms a well-defined jet at 49.9°S. FRAM displays several small, jetlike structures between 50°S and 60°S but lacks a single southern frontal jet. The volume transport in FRAM across this closed section is 185 Sv, the same as through Drake passage.

In a recent survey, *Read and Pollard* [1993] identified the STF at 38°S at the Greenwich meridian and at approximately 41°S at 30°E, with the ARF at 40°S. In their study, the PF and SAF combined into a single jet at 48°S. Calculations of geostrophic transports relative to the deepest common level gave 249.8 Sv at 33°E, in close agreement with our HASO estimate. However, this appears too high, because the transport through Drake passage (which should be approximately the same as that through the closed section south of Africa; the net flow into the Atlantic is of the order of a Sv) is approximately 134 Sv [*Whitworth and Peterson*, 1985]. Interestingly, if the transport relative to the bottom (the baroclinic component only) is calculated from FRAM, a figure of 247 Sv south of Africa is obtained, agreeing with HASO and implying net westward bottom currents south of Africa. The transport differences between FRAM and HASO must be accounted for by these deep westward bottom currents, which we have neglected by adopting a bottom reference level. For example, an average bottom current of only 0.5 cm s^{-1} across the section would be sufficient to account for the discrepancy. FRAM includes local westward bottom currents, features supported by the inverse calculation of *Olbers and Wenzel* [1989]. Although there are known to be eastward flows of Antarctic Bottom Water at some locations, this analysis, perhaps surprisingly, implies the bottom currents of the section are, on average, westward. There are also differences between FRAM and HASO in the Agulhas Current, with FRAM giving a mean transport of 90 Sv and HASO, 35 Sv (for a fuller description of the Agulhas Current in FRAM, see *Lutjeharms and Webb* [1995]).

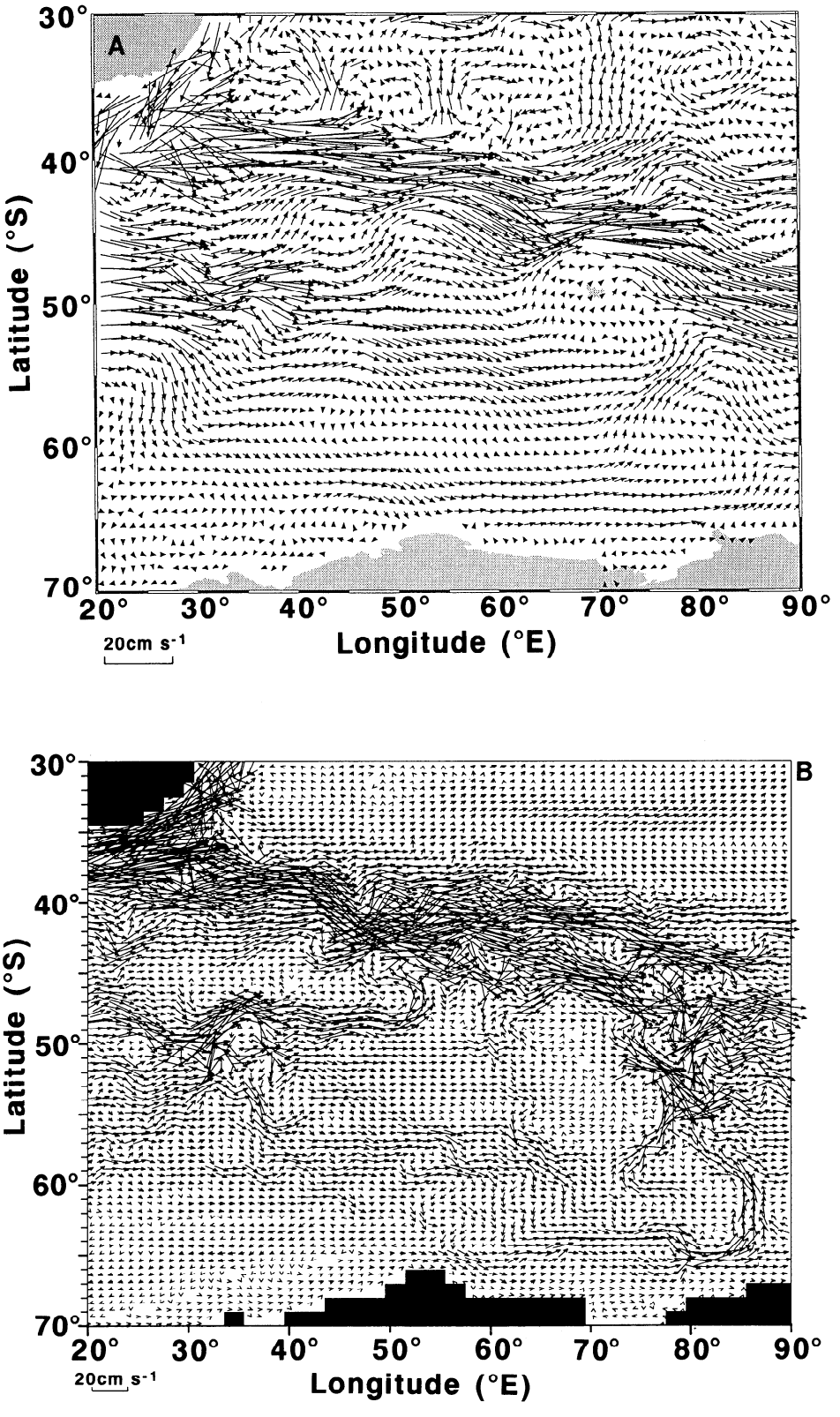

Figure 2. Surface velocity vectors from the (a) Hydrographic Atlas of the Southern Ocean (HASO) and (b) fine resolution Antarctic model (FRAM) 6-year average data set, with every second velocity vector shown for greater clarity.

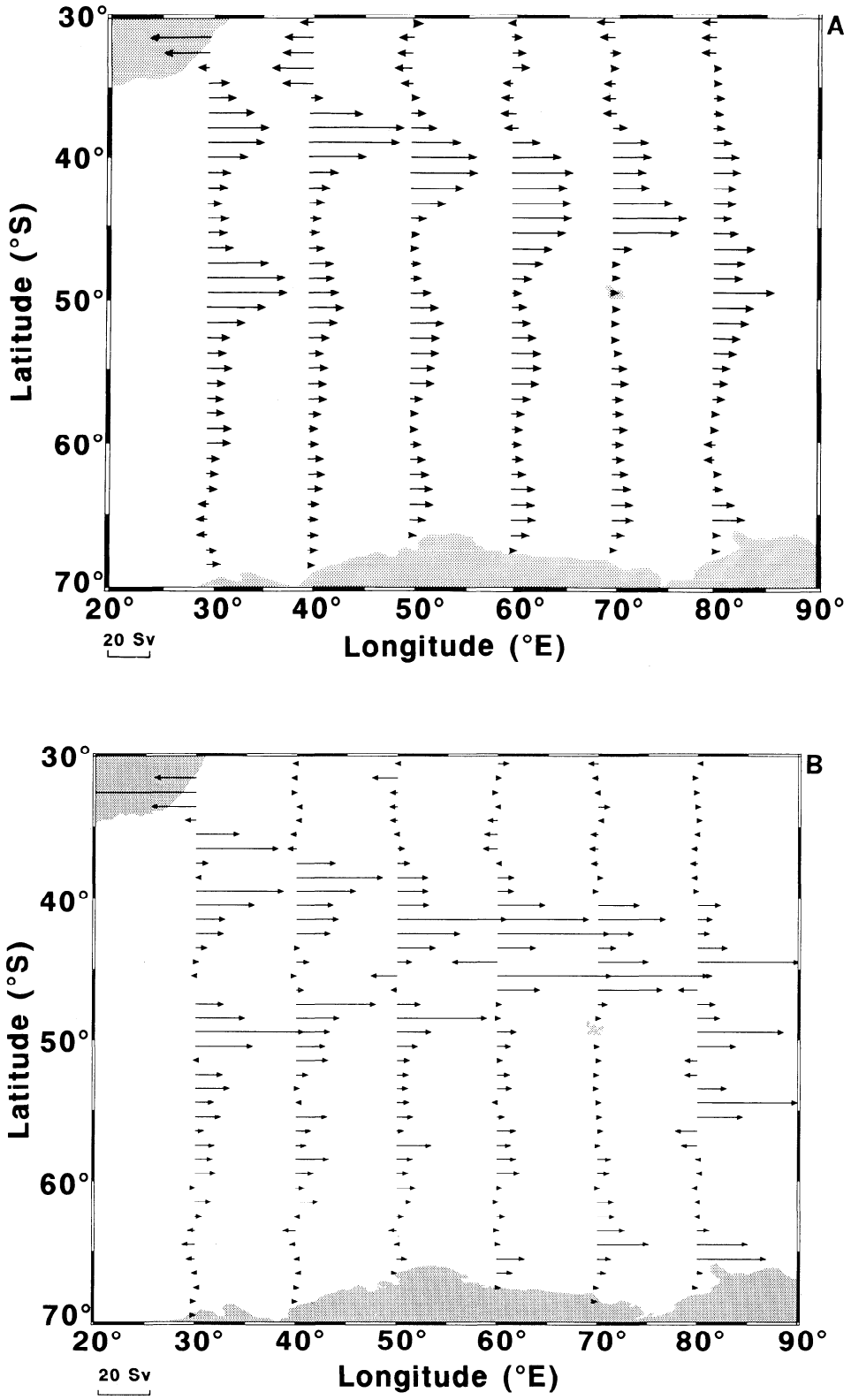

Figure 3. Zonal volume transport derived from (a) HASO and (b) the FRAM 6-year average data set.

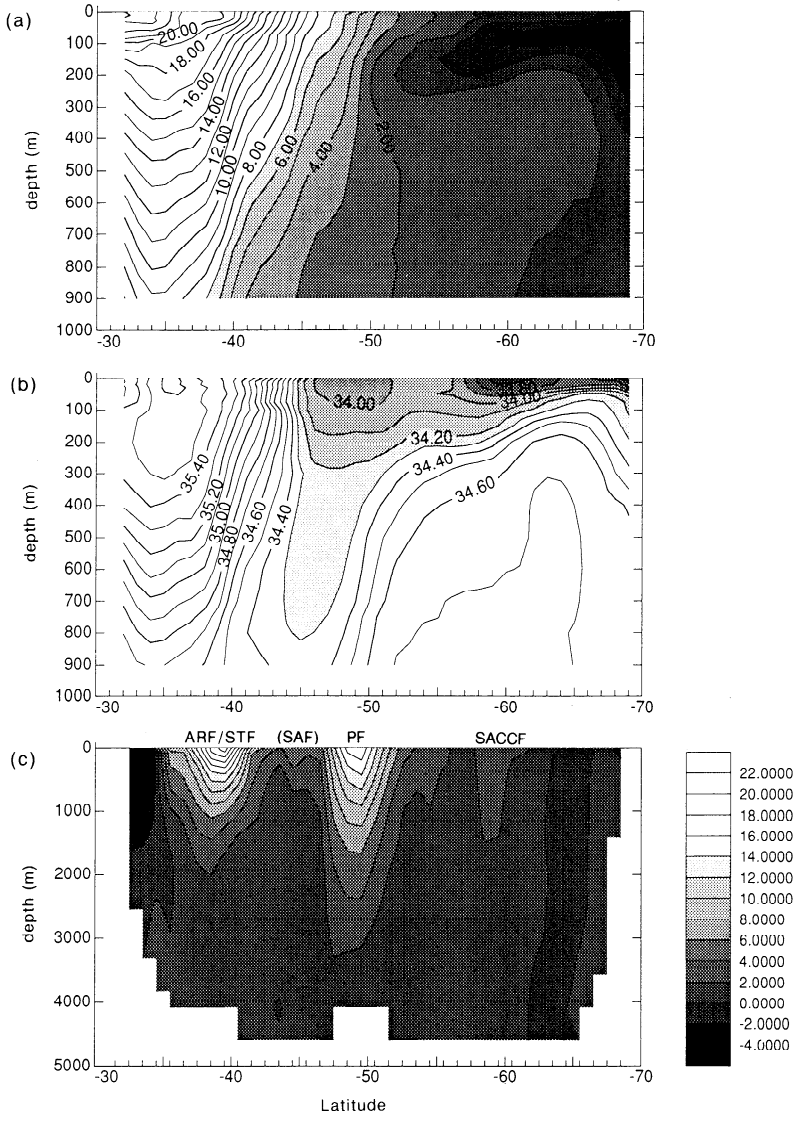

Figure 4. Section at 30°E from HASO, showing (a) potential temperature (in degrees Celsius), (b) salinity, and (c) zonal component of geostrophic velocity (centimeters per second). Eastward is positive.

Section at 40°East

At 40°E (Figures 2 and 3, individual sections not shown) the effect of bottom topography begins to be seen in the HASO data set; the SAF has apparently merged with the ARF/STF and has become the dominant frontal system, with velocities of up to 30 cm s^{-1}, whereas the PF has decreased in intensity, with a peak velocity of 11 cm s^{-1}. In FRAM the ARF and STF have merged at 38.1°S, with a peak eastward velocity of 43 cm s^{-1}. The SAF can be seen as a separate front at 41.4°S, with a velocity of 17 cm s^{-1}. Again, the PF has decreased in intensity, to 21 cm s^{-1}. In HASO the southern frontal jet has moved farther south to 62°S, appearing in FRAM at 58°S. The southern boundary is not resolvable in HASO at this longitude.

Section at 50°East

The approximate longitude of Crozet Island, where the influence of the bottom topography is pronounced, is 50°E (Figures 2, 3, and 6). There is an intense current core to the north of the island and a less pronounced frontal system to the south. In HASO the main current core lies at 40-41°S, peaking at 25 cm s^{-1} (Figure 6c), with a total transport of 105 Sv. The temperature and salinity sections (Figures 6a and 6b) suggest that the core is a convergence of the ARF (at 40°S), the STF (at 41°S), and the SAF (at about 42°S). The surface salinity minimum of the PFZ is evident just south of the SAF, the northern extent of the 2°C isotherm suggesting the subsurface expression of the PF at 49°S; though *Park et al.* [1993] suggested that the 2.5°C isotherm is a better indicator at this longitude, which would place the PF half a degree farther north. However, most of the transport (65 Sv) associated with the PF is concentrated in a jet centered around 52°S, coincident with the surface expression of the PF. The southern jet can also be seen in this section, centered at 63.3°S, with transports comparable with the PF (30 Sv). In this case the southern limits of the 1.8°C isotherm and 34.74 isohaline correspond well with the northern limit of the jet, characterizing this feature as the SACCF described by *Orsi et al.* [1995].

In FRAM (Figures 2b and 3b) the principal contributors to the main current core north of Crozet are the ARF (37-40°S),

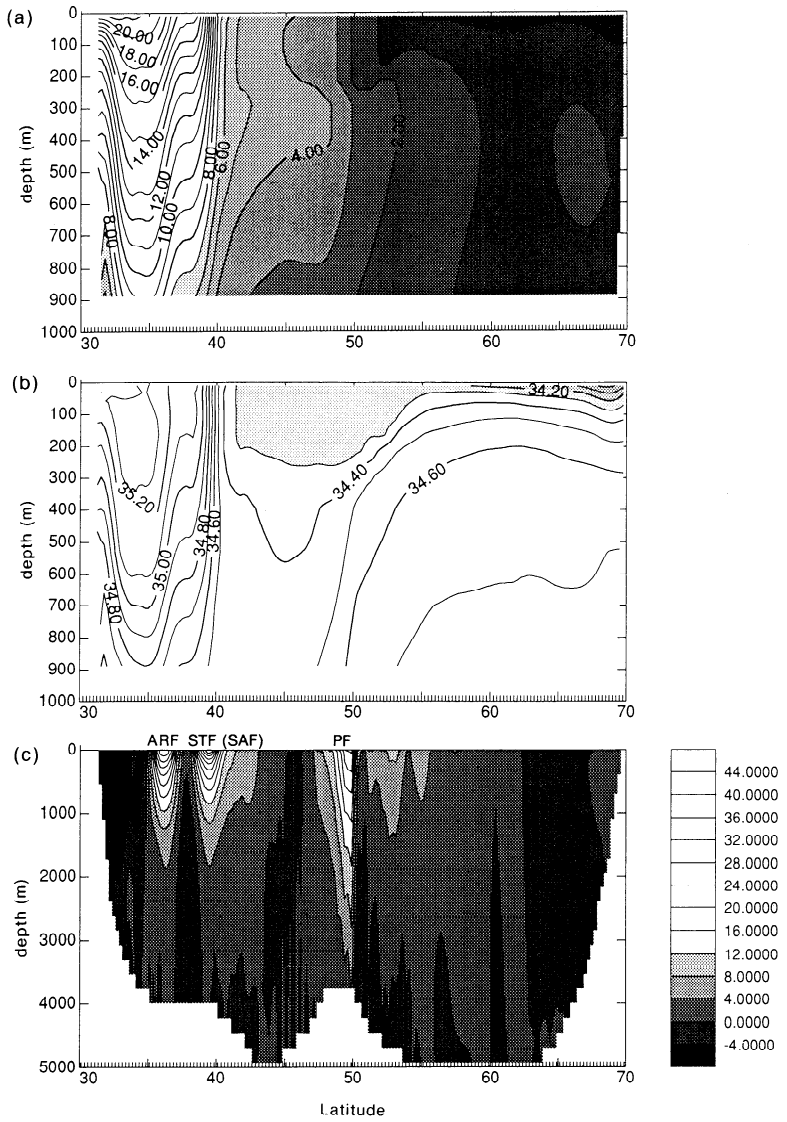

Figure 5. Section at 30°E from the FRAM 6-year average data set, showing (a) potential temperature (degrees Celsius), (b) salinity, and (c) zonal component of velocity (centimeters per second). Eastward is positive.

the STF (40-42°S), and SAF (42°S), with a total transport of 94 Sv, and velocities reaching 53 cm s^{-1}. The PF can be identified at 48°S, with several minor jets to the south. Total transports across the section from 30°S to Antarctica are 190 Sv in HASO and 220 Sv in FRAM. *Park et al.* [1993], in their SUZIL sections 1-19 (50-55°E, 35-51°S), derived current velocities of up to 95 cm s^{-1} (considerably higher than the smoothed HASO) in the ARF at 41°S, falling to 41 cm s^{-1} near the SAF. They identified the PF as a very weak phenomenon with little baroclinic shear, carrying only 7 Sv compared with 120 Sv in the main current core. This was almost certainly the subsurface expression of the PF. The sections of *Park et al.* [1993] only extended as far south as 51°S, so the presence of the surface expression of the PF could not be identified.

Section at 60°East

The 60° meridian (Figures 2, 3 and 7) is approximately midway between Crozet and Kerguelen. In HASO the main current core has widened to lie between 39 and 47°S, with a transport of 154 Sv. Temperature and salinity characteristics place the ARF, STF, and SAF at 41°S, 43°S, and 45°S, respectively. There is evidence of two maxima in the flow, the strongest being at 41°S, with a maximum velocity of 19 cm s^{-1} (Figure 7c). Comparison with the previous section shows that at 200 m the northern side of the ARF is colder (by 2°C) and less saline (by 0.2), suggesting that the strength of the ARF has decreased dramatically. The surface expression of the PF has progressed southward to 55-56°S, whereas the subsurface expression lies at 50°S. The jet associated with the surface expression of the PF has a velocity and transport about half that of the main current core. Subsurface salinity and temperature minima (Figures 7a and 7b) are those associated with the PFZ, with the subsurface salinity minimum best shown by the 34.4 isohaline. The SACCF continues to move south with increasing longitude, the maximum signal of the front now being at 64.2°S, with a velocity of 4-6 cm s^{-1} and a transport of 35 Sv. *Park et al.* [1993] placed the main ACC frontal zone between 43.7°S and 45.3°S, with a peak velocity

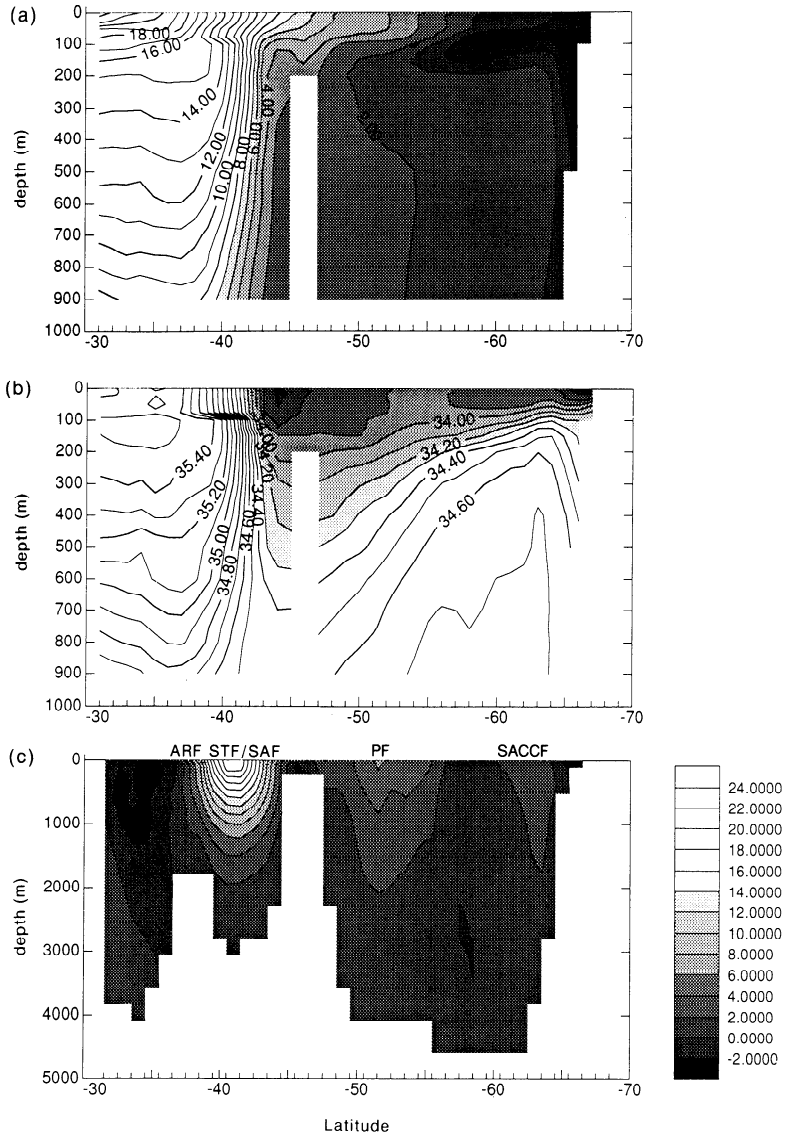

Figure 6. Same as Figure 4, but for 50°E (HASO).

of 57 cm s^{-1}, and the PF at 49.5°S, again corresponding to the subsurface expression.

FRAM locates the main current core between 37°S and 44°S, peaking at about 41.6°S, with a velocity of 34 cm s^{-1} and a total transport of 112 Sv. One significant difference between FRAM and HASO is that the major (surface expression) branch of the PF (carrying 57 Sv) in FRAM is just to the south of the main current core and to the north of the islands, at about 46°S. The SACCF is evident at 66°S in FRAM, with a transport of 19 Sv. Total transport estimates are much closer at this longitude, with FRAM giving 230 Sv across the section and HASO, 250 Sv.

Section at 70° East

The 70°E section bisects the island of Kerguelen (49°S), the Kerguelen Plateau extending southeastward (Figures 2, 3, 8, and 9). In HASO the main current core is separated into two jets, the stronger lying against the northern flank of Kerguelen, with maximum surface velocities of 27 cm s^{-1}, and a weaker jet at 39°S of 10 cm s^{-1} (Figure 8c). Transport associated with the core is 122 Sv, compared with 152 Sv for the whole section. The temperature and salinity sections (Figures 8a and 8b) suggest that the weaker front still has characteristics of the ARF, the stronger being the STF (44°S) and SAF (45°S). The eastward component of the surface expression of the PF (evident at about 56°S, Figure 2a) is weaker, as it begins to turn northward (Figure 8c), conserving potential vorticity as it passes over the relatively shallow topography of the plateau. It is clearly constrained to cross the deepest part of the plateau between 57°S, 75°E and 55°S, 80°E (compare Figures 1 and 2a, see section 4). The position of the subsurface expression of the PF is more difficult to locate, though as it appears at about 47°S at 72°E, it is likely that at 70°E it is within the main current core, to the north of Kerguelen. The SACCF is easily identifiable at 64.2°S, with an associated transport of nearly 30 Sv and velocities of about 5-6 cm s^{-1}.

The FRAM section is similar to HASO, with the main current core to the north of Kerguelen split into two structures at 41.1°S and 45.4°S, with velocities of 28 and 35 cm s^{-1} (Figure 9c) and transports of 56 and 86 Sv, respectively. The structure farthest north is the STF, the jet at 45.4°S is a combination of the SAF and surface expression of the PF,

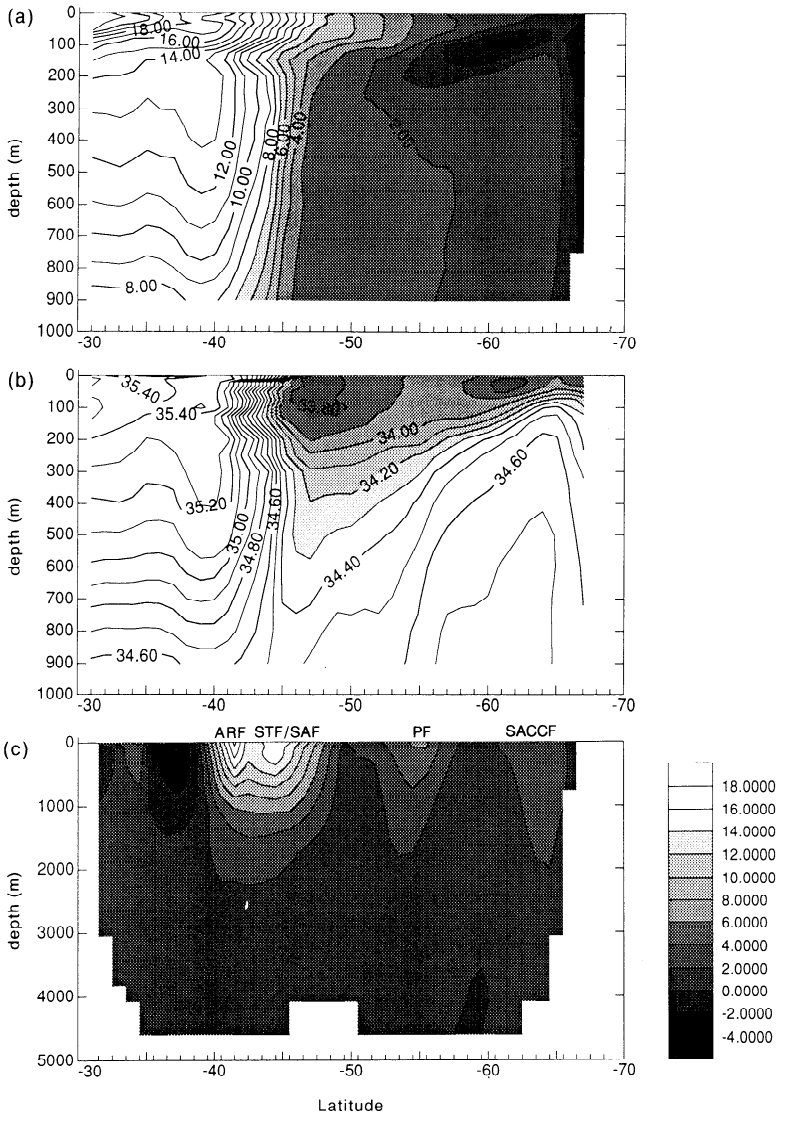

Figure 7. Same as Figure 4, but for 60°E (HASO).

which is confirmed by the temperature and salinity sections (Figure 9). The subsurface expression of the PF lies south of the surface expression (see section 4), at 47°S, and seems to be associated with little transport. A well-defined SACCF exists at 63.9°S with maximum velocities of 15 cm s^{-1}. The total transport across this section is 213 Sv, with 146 Sv flowing to the north of Kerguelen. The CTD sections from 39 to 51°S and 65 to 70°E of *Park et al.* [1993] are the closest in position to the HASO/FRAM sections. They observed one main current core at 45°S, which they identified as a combination of the SAF and STF, but no PF.

Section at 80°East

In HASO, three frontal jets at 41°S, 46°S, and 49°S can be identified (Figures 2 and 3; individual sections not shown). The temperature and salinity properties would place the STF between 43 and 45°S; the temperature gradient between 12 and 16°C at 200 m seems no longer a good indicator of the position of the ARF. The 12°C isotherm, however, exists at 40°S, suggesting that the jet at 41°S is the STF modified by the ARF, even at this longitude. The jets at 46°S and 49°S are the SAF and PF, respectively. At this longitude the subsurface and surface expressions of the PF coincide, and as in the 30°E section, the PF is reestablished as the strongest front having surface velocities reaching 17 cm s^{-1} compared with 9 and 10 cm s^{-1} in the STF and SAF. The jet associated with the SACCF passes through the deep channel of the Princess Elizabeth Trough (PET) south of the Kerguelen Plateau, having an associated velocity and transport of 6 cm s^{-1} and 20 Sv, respectively.

FRAM has five well-defined frontal systems at this longitude, from north to south, as follows: the STF at 41°S, with velocities of 14 cm s^{-1}, the SAF at 44°S (34 cm s^{-1}); two expressions of the PF at 49.6°S (surface expressions) and 54.4°S (subsurface expression), with associated velocities of 30 and 26 cm s^{-1} ; and the SACCF at 65.1°S, with a velocity of 19 cm s^{-1}.

Park et al. [1993] carried out a CTD section from 37°S, 70°E to 51°S, 79°E. They observed a frontal zone between 44.5°S and 45.3°S composed of the STF and the SAF and a secondary feature between 46°S and 47°S, which they concluded was a branch of the SAF. This was quite different than the situation observed in 1987 [*Park et al.*, 1991], where

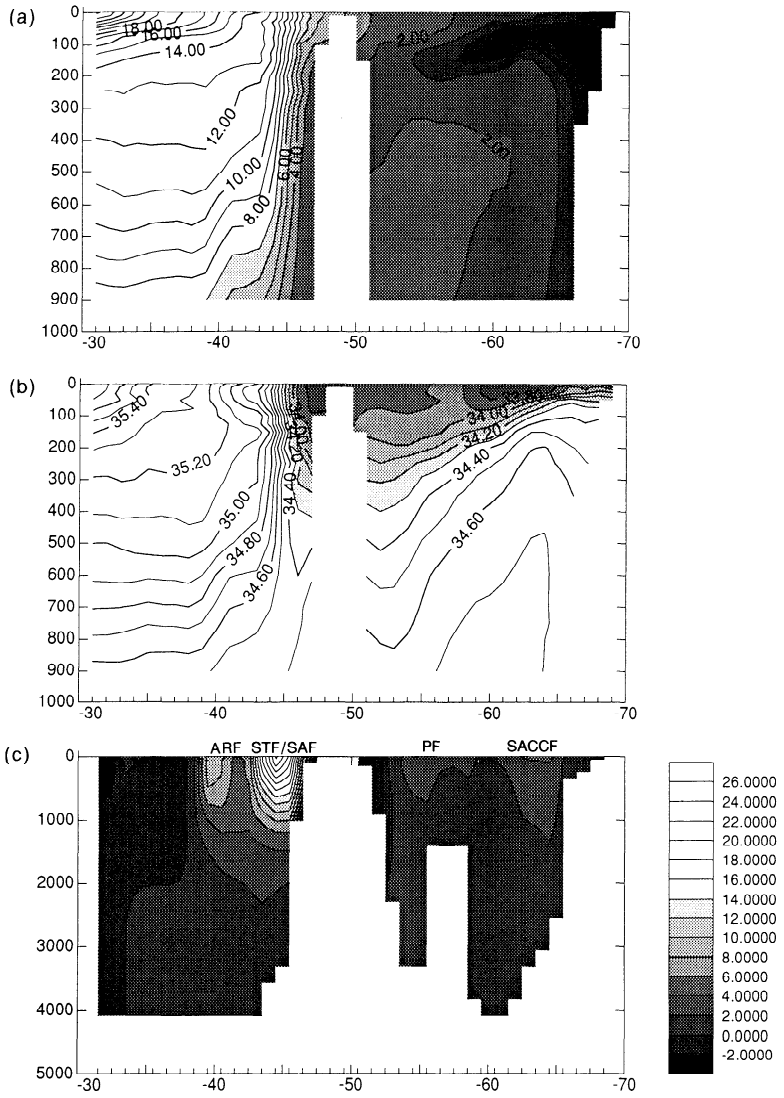

Figure 8. Same as Figure 4, but for 70°E (HASO).

only one frontal zone between 44.7°S and 46.7°S existed, suggesting temporal variability of the frontal structure in this area.

4. Discussion

This analysis has shown the complicated nature of the frontal jet structure in the south Indian Ocean. A summary of the positions and branching of the ACC fronts deduced in our study from HASO is shown schematically in Figure 1. The bottom topography, particularly the Kerguelen Plateau, has a major effect on the ACC structure.

The Confluence of the ARF, STF, and SAF

Park et al. [1993] showed that the ACC to the north of Crozet and Kerguelen has a structure peculiar to the region, with the bulk of the transport concentrated in a core formed by the confluence of the ARF, STF, and SAF. This confluence, sometimes referred to as the Crozet Front, has remarkably pronounced surface temperature and salinity differences of up to 11°C/1.8 across it [*Belkin and Gordon*, 1996]. However, it is probably inaccurate to talk of a single Crozet Front, as although some cross-frontal mixing will occur, the properties of the three frontal jets would probably be discernible if sufficiently high-resolution data were available. Using the relatively low resolution data in our study, the ARF, STF, and SAF merge to form a single current core at about 40°E. This core moves southward and eastward, reaching its maximum intensity north of Crozet. Between Crozet and Kerguelen the core widens, separating into its constituent frontal jets. To the north of Kerguelen the STF and SAF become indistinguishable in this analysis. In HASO (unlike FRAM) the ARF, though weak, forms a separate frontal jet which meanders northward to 39°S. East of Kerguelen, the ARF again merges with the STF (itself separating from the SAF), a similar situation to that seen by *Belkin and Gordon* [1996].

FRAM and HASO agree well in terms of the structure of the ACC current core. The principal difference is that the ARF is discernible up to 75°E in HASO but only 50°E in FRAM. Previous studies have demonstrated that the ARF can be traced as far as 73°E [*Belkin and Gordon*, 1996]. It is the modification of the water characteristics of the ARF as it

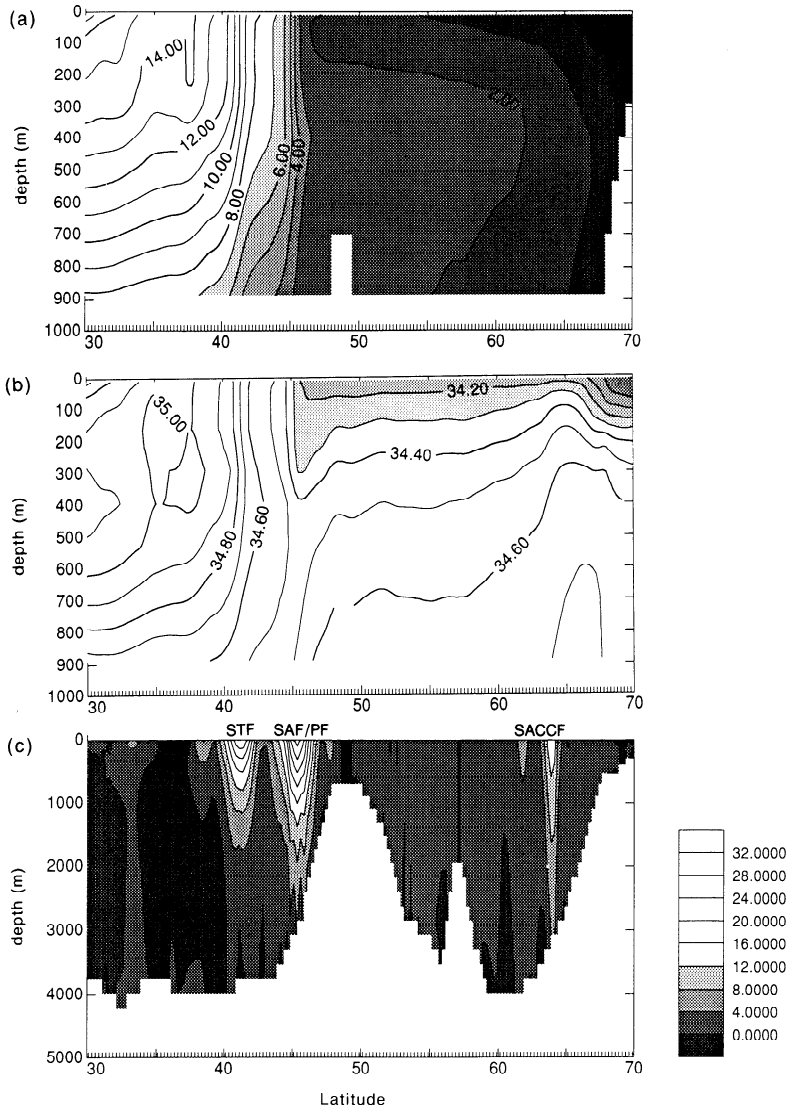

Figure 9. Same as Figure 5, but for 70°E (FRAM).

progresses eastward that renders the identification increasingly difficult. A reason for this change may be the northward branching of the Agulhas frontal jet [*Belkin and Gordon*, 1996; *Stramma*, 1992]. *Stramma* [1992] noted various northward branches separating from the frontal jet (referred to as the South Indian Ocean Current in his paper). These northward transports are also apparent in the HASO data set (Figure 2a) at approximately 40, 53 and 69°E but are absent in the FRAM output.

The Polar Front

At 30°E the PF is composed of a single frontal jet at 49°S. Moving eastwards, the front passes between Crozet and the Ob'Lena (Conrad) rise. At about 50°E, however, the surface and subsurface expressions of the PF are no longer coincident. In HASO the surface expression of the PF, carrying most of the transport, moves southeastward, reaching 56°S, 6° farther south than at the Greenwich meridian, before being forced northeastward through the col in the Kerguelen Plateau. Here velocities reach 7 cm s^{-1} in HASO and 20 cm s^{-1} in the dynamically sharpened FRAM, with respective transports of 14 and 22 Sv, confirming the southern expression of the PF as a significant contributor to the volume flux of the ACC at this longitude. HASO and FRAM differ, in that most of the transport in FRAM is associated with the more northerly jet, passing between Crozet and Kerguelen and forming a frontal system just to the south of the main circumpolar transport. In HASO the subsurface expression of the PF is associated with little or no geostrophic shear west of Kerguelen. To the east of Kerguelen, however, the surface and subsurface expressions of the PF merge, in both FRAM and HASO, as the more southerly expression of the PF moves strongly northward.

It is evident from the literature that the PF is a nonstatic feature, exhibiting considerable spatial and temporal variability, especially in the region of Kerguelen. In part, this may be attributable to inconsistencies in the definition of the boundary characteristics of the PF (e.g., northern limit of 2°C isotherm at 200 m, the northern boundary of Antarctic waters). Its position has been reported to the north of Kerguelen [e.g., *Belkin and Gordon*, 1996] at the latitude of Kerguelen [e.g., *Park et al.*, 1993], between Kerguelen and Heard Island [e.g., *Macintosh*, 1946], or south of Heard Island (for a fuller

discussion, see *Klyausov* [1990]). The southward excursion of the surface (in HASO) expression of the PF is interesting. This splitting of the surface and subsurface expressions may have been observed in other parts of the ACC, especially Drake passage [e.g., *Roether et al.*, 1993], but usually, the components remain much closer. A close examination of the drifter plots of *Hofmann* [1985, Figure 6d] suggests a frontal jet passing through the col in the Kerguelen plateau, as do the results of *Mantyla and Reid* [1995, Figure 7]. Further support can be found in a series of closely spaced ($^1/_4°$ of latitude) expendable bathythermographs (XBTs) deployed during RRS *Discovery* cruise 207 [*Dickson*, 1995]. The reason for the splitting of the surface and subsurface expressions of the PF is not clear. However, the authors suggest the following scenario. Figure 10 gives TS plots of every second degree of latitude along 75°E from 47°S to 57°S, 75°E being chosen, because it crosses both the surface and subsurface expressions of the PF. There is little change in the TS characteristics between 55°S and 49°S but comparatively large changes between 57°S and 55°S (the surface expression of the PF) and 49°S and 47°S (the subsurface expression of the PF). If we look at the positioning of the WW layer (corresponding to a temperature and salinity minimum on the TS plot), it can be seen that the WW layer minimum drops from 100 to 150 m at the surface expression, then gradually subducts over the next 6° of latitude by 50 m. At the subsurface expression of the PF it undergoes a further change in depth to 250 m. Thus the surface expression of the PF will not coincide with the subsurface expression, because the WW layer sinks in two distinct places. This would also explain why FRAM, which lacks seasonal thermohaline forcing and therefore a WW layer, is incorrect in its positioning of the subsurface expression of the PF, because it is clearly wrong in the surface waters in the south.

The Southern ACC Front

This study has shown the importance of the front termed the Southern ACC Front by *Orsi et al.* [1995]. This feature has been repeatedly observed near the southern flank of Drake passage and at 52°S at the Greenwich Meridian by *Whitworth and Nowlin* [1987]. In HASO, between 20°E and 30°E, the SACCF/ southern boundary (see 30°E section) moves from about 52°S to 60°S, the strong southward motion suggested by *Deacon* [1979] and modeled by *Gouretski and Danilov* [1993]. It then extends southeastward, reaching 64.2°S at 55°E before being steered eastward along the Antarctic shelf, reaching its maximum velocity in PET. In FRAM a single SACCF is difficult to distinguish until 50-60°E, after which it follows a similar pattern to HASO. East of PET, HASO has the SACCF moving northward to about 60°S, while FRAM has a much stronger northward displacement, moving the SACCF northwestward along the eastern side of the Kerguelen plateau to about 55°S. *Speer and Forbes* [1994] observed a northward excursion of the SACCF to about 58-59°S just to the east of the Kerguelen plateau, suggesting that FRAM may, in fact, give a better indication of the northward extent of the SACCF than HASO. The SACCF is the only ACC front that does not separate distinct surface water masses [*Orsi et al.*, 1995] and therefore seems mainly to be a subsurface feature. Therefore, despite being wrong in the surface layers this far south, FRAM does a reasonable job of resolving the SACCF. Recent surveys carried out in PET confirm the presence of the SACCF [e.g., *Speer and Forbes*, 1994]. On both the RRS *Discovery* cruise 200 (February-March 1993) [*Dickson*, 1993] and a recent cruise on the *Aurora Australis* (N. Bindoff, personal communication, 1995) an eastward flowing jet of approximately 10 cm s^{-1} (relative to the bottom) was observed with the characteristics of the SACCF.

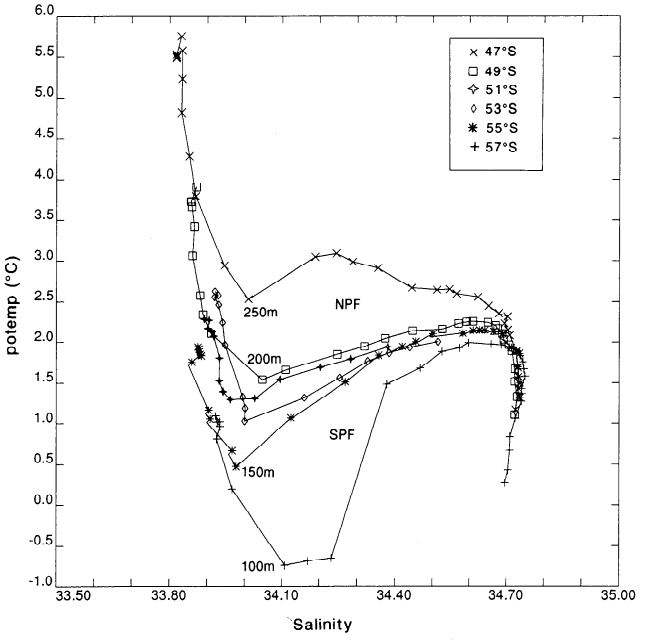

Figure 10. TS plots along 75°E. Data are shown every second degree of latitude from 47°S to 57°S.

Other Features

Interestingly, there is little evidence in either FRAM or HASO for the narrow, westward flowing Antarctic Coastal Current (or Antarctic Slope Front) [*Jacobs*, 1991]. Density changes associated with the front are principally temperature controlled, and as the temperature minimum is absent in FRAM, there is no mechanism to drive an Antarctic Coastal Current. In HASO, ice cover may have prevented sampling and/or the density of observations are simply insufficient this close to the continent. Both FRAM and HASO indicate a small cyclonic gyre in the area of Prydz Bay and the Amery Ice Shelf at 75°E. HASO also has an anticyclonic gyre between 30 and 40°S and 75 to 85°E. FRAM suggests the presence of the North Subtropical Front (a feature discussed by *Belkin and Gordon* [1996]) at about 33°S, between 60 and 90°E, a feature absent in HASO. Both Figures 2 and 3 indicate a cyclonic circulation south of 60°S at 30°E and 40°E. This agrees with the analysis of *Orsi et al.* [1993], who consider it as one of the two eastward extensions of the Weddell Gyre circulation.

Gordon et al. [1978] examined geostrophic surface velocities relative to 1000 dbar, using data from the *Eltanin* and selected *Discovery* and International Geophysical Year (IGY) stations. Though coarser in resolution (1° by 2°, with fewer data points), reexamination of *Gordon et al.* [1978, Figure 2b] shows features in common with this work, namely, the current core and the southward excursion of the PF. The SACCF, however, is not evident, though there are significant data gaps south of 60°S, making identification of the front difficult. Despite a shallow reference layer, their surface geostrophic currents are of similar direction to ours referenced

to the seabed, implying our neglect of bottom currents has not unduly biased the results.

Overall, it is pleasing how well FRAM and HASO agree. Differences mainly occur because of the absence of a barotropic component in HASO, FRAM's poor bathymetry, or the lack of seasonal thermohaline forcing or sea ice processes in FRAM. The bathymetric effect is thought to be the major cause of discrepancies such as the multiplicity and incorrect positioning of the jets in FRAM [*Grose et al.*, 1995; *Lutjeharms and Webb*, 1995]. The smoothing of the bathymetry to a 1° x 1° grid was designed to prevent numerical instabilities. In the deep ocean the vertical distance between depth levels in FRAM is approximately 230 m, therefore the flow experiences much larger step changes in topography than would really be the case [*Grose et al.*, 1995]. Further discrepancies occur south of 50°S, with the omission of seasonal surface temperature forcing and sea ice processes in FRAM, the major difference being in the incorrect positioning of the surface expression of the PF in FRAM, because of the absence of a WW layer. Clearly, using more realistic topography and correctly modeling the upper few hundred meters of the water column would improve the performance of models such as FRAM.

5. Summary

Recently, there has been a great deal of interest in this area of the south Indian Ocean, yet in comparison to the well studied Drake passage region, the circumpolar current structure is poorly understood. Our study has examined frontal jets as revealed by surface velocities (relative to the bottom) and volume transports and compared them with frontal positions determined from temperature and salinity characteristics. We have confirmed the existence of the ACC current core to the north of Crozet and Kerguelen and discussed the structure of jets farther south. The evident separation of the surface and subsurface expressions of the PF helps reconcile confusion in the literature as to the location of the front. A mechanism for the splitting of expressions of the PF is not clear; it may be topographic, but this is far from obvious. Clearly, the col in the Kerguelen Plateau acts as a strong control on transport. Finally, this analysis provides independent confirmation of the presence of the SACCF [*Orsi et al.*, 1995], highlighting its importance in contributing a significant proportion (up to 30 Sv) of the eastward volume transport of the ACC. Overall, it is pleasing how well HASO and FRAM agree in the locations and transports of the jets.

Acknowledgments. We are grateful to Victor Gouretski and to D. Olbers' group at the Alfred-Wegener Institute for making the hydrographic data from their atlas available and to David Webb and the FRAM group at IOSDL for access to their model output. M.D.S. acknowledges the support of a CASE Ph.D. studentship jointly between the U.K. Natural Environment Research Council and MAFF, Lowestoft. We appreciate the detailed and helpful comments of the anonymous reviewers of this manuscript.

References

Belkin, I. M., and A. L. Gordon, Southern Ocean fronts from the Greenwich Meridian to Tasmania, *J. Geophys. Res.*, in press, 1996.

Clifford, M. A., A descriptive study of the zonation of the Antarctic Circumpolar Current and its relation to wind stress and ice cover,. MS thesis, 93 pp., Texas A&M Univ. College Station, 1983.

Deacon, G. E. R., The hydrology of the Southern Ocean, *Discovery Rep. 15*, pp. 3-122, 1937.

Deacon, G. E. R., The Weddell Gyre, *Deep Sea Res., Part A, 26*, 981-995, 1979.

Dickson, R. R., Report of RRS Discovery cruise 200, 6 February-18 March 1993, Circulation and structure on the Southern Ocean between 20°E and 90°E and 40°S and 65°S, Ministry of Agric., Fish., and Food Dir. of Fish. Res., Lowestoft, U.K., 1993.

Dickson, R. R., Report of RRS Discovery cruise 207, 19 February-31 March 1994, Circulation and structure on the Southern Ocean between 20°E and 90°E and 40°S and 65°S, Ministry of Agric., Fish., and Food Dir. of Fish. Res., Lowestoft, U.K., 1995.

Gordon, A. L., E. Molinelli, and T. Baker, Large-scale relative dynamic topography of the Southern Ocean, *J. Geophys. Res.*, *83*(C6), 3023-3032, 1978.

Gordon, A. L., J. R. E. Lutjeharms, and M.L. Gründlingh, Stratification and circulation at the Agulhas Retroflection, *Deep Sea Res., Part A, 34*, 565-599, 1987.

Gouretski, V. V., and A. I. Danilov, Weddell Gyre: Structure of the eastern boundary, *Deep Sea Res., Part I, 40*, 561-582, 1993.

Grose, T. J., J. A. Johnson, and G.R. Bigg, A comparison between the FRAM (Fine Resolution Antarctic Model) results and observations in the Drake Passage, *Deep Sea Res, Part I, 42*, 365-388, 1995.

Hellerman, S., and M. Rosenstein, Normal monthly wind stress over the World Ocean with error estimates, *J. Phys. Oceanogr., 13*, 1093-1104, 1983.

Hofmann, E. E., The large-scale horizontal structure of the Antarctic Circumpolar Current from FGGE drifters, *J. Geophys. Res.*, *90*(C4), 7087-7097, 1985.

Jacobs, S. S., On the nature and significance of the Antarctic Slope Front, *Mar. Chem., 35*, 9-24, 1991.

Jacobs, S. S., and D. T. Georgi, Observations on the southwest Indian/Antarctic Ocean, in *A Voyage of Discovery*, pp. 43-84, Pergamon Press, Oxford, 1977.

Killworth, P. D., An equivalent-barotropic mode in the Fine Resolution Antarctic Model, *J. Phys. Oceanogr., 22*, 1379-1387, 1992.

Klyausov, A. V., Position of the South Polar Front near Kerguelen and Heard Islands in the Autumn of 1987, *Oceanology, Engl. Transl., 30*(2), 142-148, 1990.

Levitus, S., Climatological atlas of the world ocean, *NOAA Prof. Pap. 13*, 173 pp., U.S. Govt. Print. Off., Washington, D.C., 1982.

Lutjeharms, J. R. E., and H. R. Valentine, Southern Ocean thermal fronts south of Africa, *Deep Sea Res.*, Part A, *31*, 1461-1475, 1984.

Lutjeharms, J. R. E., and D. J. Webb, Modelling the Agulhas Current system with FRAM (Fine Resolution Antarctic Model, *Deep Sea Res, Part I, 42*, 523-551, 1995.

Macintosh, N. A., The Antarctic Convergence and the distribution of surface temperatures in antarctic water, *Discovery Rep. 23*, pp. 171-212, 1946.

Mantyla, A. W., and J. L. Reid, On the origins of deep and bottom waters of the Indian Ocean, *J. Geophys. Res, 100*(C2), 2417-2439, 1995.

Nowlin, W. D., and M. Clifford, The kinematic and thermohaline zonation of the Antarctic Circumpolar Current at Drake Passage, *J. Mar. Res., 40*, 481-507, 1982.

Nowlin, W. D., and J. M. Klinck, The physics of the Antarctic Circumpolar Current, *Rev. Geophys. 24*(3), 469-491, 1986.

Nowlin, W. D., T. Whitworth, and R. D. Pillsbury, Structure and transport of the Antarctic Circumpolar Current at Drake Passage from short-term measurements, *J. Phys. Oceanogr., 7*, 788-802, 1977.

Olbers, D., and M. Wenzel, Determining diffusivities from hydrographic data by inverse methods with applications to the circumpolar current, in *Oceanic Circulation Models: Combining Data and Dynamics*, edited by D. L. T. Anderson and J. Willebrand, pp. 95-139, Kluwer Acad., Norwell, Mass., 1989.

Olbers, D., V. Gouretski, G. Seiβ, and J. Schroter, Hydrographic Atlas of the Southern Ocean, 82 pp., Alfred Wegener Inst. for Polar and Mar. Res., Bremerhaven, Germany, 1992.

Orsi, A. H. , T. Whitworth III, and W. D. Nowlin Jr., On the circulation and stratification of the Weddell Gyre, *Deep Sea Res., Part I, 40*, 169-203, 1993.

Orsi, A. H. , T. Whitworth III, and W. D. Nowlin Jr., On the meridional extent and fronts of the Antarctic Circumpolar Current, *Deep Sea Res., Part I, 42*, 641-673, 1995.

Ostapoff , F., The salinity distribution at 200 metres and the Antarctic Frontal zones, *Dtsch. Hydrogr. Z., 15*, 133-141, 1962.

Park, Y.-H., L. Gamberoni, and E. Charriaud, Frontal structure and transport of the Antarctic Circumpolar Current in the South Indian Ocean sector 40-80 E, *Mar. Chem., 35*, 45-62, 1991.

Park, Y.-H., L. Gamberoni, and E. Charriaud, Frontal structure, water masses and circulation in the Crozet Basin, *J. Geophys. Res., 98*(C7), 12,361-12,385, 1993.

Peterson, R. G., and L. Stramma, Upper-level circulation in the South Atlantic ocean, *Prog. Oceanogr., 26*, 1-73, 1991.

Read, J. F., and R. T. Pollard, Structure and transport of the Antarctic Circumpolar Current and Agulhas Return Current at 40 East, *J. Geophys. Res., 98*(C7), 12,281-12,295, 1993.

Read, J. F., R. T. Pollard, A. I. Morrison, and C. Symon, On the southerly extent of the Antarctic Circumpolar Current in the Southeast Pacific, *Deep Sea Res., Part II, 42*, 933-954, 1995.

Robertson, I. E., and A. J. Watson, A summertime sink for atmospheric Carbon Dioxide in the Southern Ocean between 80°W and 80°E, *Deep Sea Res., Part II, 42*, 1081-1091, 1995.

Roether, W., R. Schlitzer, A. Putzka, P. Beining, K. Bulsiewicz, G. Rohardt, and F. Delahoyde, A chlorofluoromethane and hydrographic section across Drake Passage: Deep water ventilation and meridional transport, *J. Geophys. Res., 98*(C8), 14,423-14,435, 1993.

Sievers, H. A., and W. D. Nowlin, The stratification and water masses at Drake Passage, *J. Geophys. Res., 89*(C6), 10,489-10,514, 1984.

Speer, K. G., and A. Forbes, A deep western boundary current in the South Indian Basin, *Deep Sea Res., Part I, 41*, 1289-1303, 1994.

Stramma, L., The South Indian Ocean Current, *J. Phys. Oceanogr., 22*, 421-430, 1992.

The FRAM group, Initial results from a fine resolution model of the Southern Ocean, *Eos Trans. AGU*, 72, 169, 174-175, 1991.

Webb, D. J., A simple model of the effect of the Kerguelen Plateau on the strength of the Antarctic Circumpolar Current, *Geophys. Astrophys. Fluid Dyn., 70*, 57-84, 1993.

Webb, D. J., P. D. Killworth, A. Coward, and S. Thompson, *The FRAM Atlas of the Southern Ocean*, 67 pp., Nat. Environ. Res. Counc., Swindon, England, 1991.

Whitworth, T., III, and W. D. Nowlin, Water masses and currents of the Southern Ocean at the Greenwich Meridian, *J. Geophys. Res., 92*(C6), 6462-6476, 1987.

Whitworth, T., III, and R. G. Peterson, Volume transport of the Antarctic Circumpolar Current from bottom pressure measurements, *J. Phys. Oceanogr, 15*, 810-816, 1985.

J. Brown, Ministry of Agriculture, Fisheries and Food, Directorate of Fisheries Research, Fisheries Laboratory, Lowestoft NR33 0HT, England (e-mail: j.brown@dfr.maff.gov.uk)

K. J. Heywood and M. D. Sparrow, School of Environmental Sciences, University of East Anglia, Norwich NR4 7TJ, England (e-mail: m.sparrow@uea.ac.uk; k.heywood@uea.ac.uk)

D. P. Stevens, School of Mathematics, University of East Anglia, Norwich NR4 7TJ, England (e-mail: d.stevens@uea.ac.uk)

(Received September 7, 1994; revised September 7, 1995; accepted October 30, 1995.)